

# The impact of the reduced speed of light approximation on the post-overlap neutral hydrogen fraction in numerical simulations of the epoch of reionization

P. Ocvirk<sup>1</sup>, D. Aubert<sup>1</sup>, J. Chardin<sup>1</sup>, N. Deparis<sup>1</sup>, and J. Lewis<sup>1</sup>

Observatoire astronomique de Strasbourg, Université de Strasbourg, 11 rue de l'Université, 67000 Strasbourg, France  
e-mail: pierre.ocvirk@astro.unistra.fr

Typeset December 3, 2024; Received / Accepted

## ABSTRACT

**Context.** The reduced speed of light approximation is used in a variety of simulations of the Epoch of reionization and galaxy formation. Its popularity stems from its ability to drastically reduce the computing cost of a simulation, by allowing the use of larger, and therefore fewer timesteps to reach a solution. It is physically motivated by the fact that ionization fronts rarely propagate faster than some fraction of the speed of light. However, no *global* proof of the physical validity of this approach is available and possible artefacts resulting from this approximation therefore need to be identified and characterized to allow its proper use.

**Aims.** In this paper we investigate the impact of the reduced speed of light approximation on the predicted properties of the intergalactic medium.

**Methods.** To this end we use fully coupled radiation-hydrodynamics RAMSES-CUDATON simulations of the epoch of reionization.

**Results.** We find that reducing the speed of light by a factor 5 (20, 100) leads to overestimating the post-reionization average volume-weighted neutral hydrogen fraction by a similar factor  $\sim 5$  (20, 100) with respect to full speed of light simulations. We show that the error is driven by the hydrogen - photon chemistry by considering the analytical solution for a strongly ionized hydrogen gas in photo-ionization equilibrium. In this regime, reducing the speed of light has the same effect as artificially reducing the photon density or the reaction cross-section and leads to an underestimated ionizing intensity. We confirm this interpretation by running additional simulations using a reduced speed of light in the photon propagation module, but keeping this time the true speed of light in the chemistry module. With this setup, the post-reionization neutral hydrogen fractions converge to the true value, which validates our explanation. Our resolution study suggests that increasing spatial resolution may yield lower ionizing halo escape fractions, which in turn would result in higher post-overlap volume-averaged neutral fractions.

**Key words.** Epoch of Reionization, radiative transfer, thermochemistry, intergalactic medium

## 1. Introduction

The epoch of reionization (hereafter EoR), is the period during which the ultra-violet light of the first stars and galaxies ionized the intergalactic medium (hereafter IGM), in expanding HII regions of increasing size, finally merging together to produce the almost uniformly ionized IGM we see today. This process ended about 1 billion years after the Big Bang, and is tightly coupled to the formation and growth of galaxies during this period. This period is the focus of a broad effort throughout the astrophysical community, aiming to understand in detail the timeline and identify the main sources contributing to the reionization of the Universe. In order to interpret the current data, and to prepare for the wave of new data expected from current and future redshifted 21cm experiments (e.g. LOFAR, MWA, HERA, SKA), and upcoming space observatories such as JWST, accurate models of galaxy formation during the epoch of reionization are required. Such models also have implications for near-field cosmology, as it has been shown that the reionization history of the local group may affect the properties of its population of low-

mass galaxies (Ocvirk & Aubert 2011; Ocvirk et al. 2013, 2014; Gillet et al. 2015).

Modelling the epoch of reionization and its sources is a notoriously difficult problem. On one hand, large boxes in the 100 Mpc or more are required in order to properly sample the variety of environments and rare large voids or early massive galaxies or galaxy clusters, such as in the cosmic dawn simulation suites Ocvirk et al. (2016, 2018); Aubert et al. (2018). On the other hand, very high spatial resolution, down to the parsec scale, is necessary to describe the interstellar medium (hereafter ISM) of galaxies, and the complex processes it drives and reacts to, such as star formation, supernova feedback, and the ionizing escape fraction (Geen et al. 2016; Trebitsch et al. 2017; Gavagnin et al. 2017; Butler et al. 2017; Costa et al. 2018). The combination of large volume and high spatial resolution makes numerical simulations of galaxy formation during the EoR extremely challenging in principle, and computationally costly with the rich set of physics required.

In particular, ionizing radiation is a key process in these simulations, both for its impact in reionizing the Universe, and for the additional feedback it provides, and is espe-

cially costly to model. Two main classes of solutions have been adopted for treating hydrogen-ionizing radiation. Ray-casting algorithms involve sampling the radiation field produced by each source by a Monte-Carlo technique and follow each photon packet through the computational domain and its interaction with the hydrogen gas (Semelin et al. 2007; Baek et al. 2009; Pawlik & Schaye 2008). Another popular solution consists in considering the photons as a fluid and using the M1 closure relation (Levermore 1984; Dubroca & Feugeas 1999; Ripoll et al. 2001; Audit et al. 2002; González et al. 2007; Aubert & Teyssier 2008, 2010). This approach has led to the development of fully coupled radiation-hydrodynamics (hereafter RHD) galaxy formation codes, such as RAMSES-CUDATON (Ocvirk et al. 2016, 2018), EMMA (Aubert et al. 2015), and RAMSES-RT (Rosdahl et al. 2013). In these codes, the radiative timestep is set by the Courant condition, and is typically 100-1000 times shorter than the hydrodynamical timestep of the simulation. This simply reflects the fact that light propagation is much faster than any other process in this framework. This alone makes full RHD simulations very expensive. While some authors have alleviated this problem by accelerating the radiative transfer (hereafter RT) module using GPUs<sup>1</sup> (Aubert & Teyssier 2010; Aubert et al. 2015; Ocvirk et al. 2016, 2018), others have resorted to the so-called “reduced speed of light” approximation (hereafter RSL), in order to bring the radiative timestep closer to the hydrodynamic timestep and reduce the overhead due to RT (Kimm & Cen 2013; Rosdahl et al. 2013; Aubert et al. 2018). This can drastically reduce the RT computing time. As a consequence, RSL is extremely popular and has allowed groups to perform simulations which would be impossible using the true speed of light. Using a reduced speed of light may appear justified in dense regions (in particular in the ISM), where the ionization front (I-front) is much slower than the real speed of light. However, beyond this, no clear proof of the global physical validity of this approach has ever been provided. For instance, in optically thinner regions of average cosmic density or voids, ionization fronts may be faster than the reduced speed of light used, and the timing and geometry of reionization could be affected (Bauer et al. 2015; Gnedin 2016; Deparis et al. 2019). More recently, Katz et al. (2017, 2018); Rosdahl et al. (2018) have introduced and deployed the variable speed of light (hereafter VSL) formalism with adaptive mesh refinement simulations, in which the speed of light is divided by a factor of 2 at each additional spatial refinement level. This allows to keep the speed of light close or equal to its true value on the base grid, where ionization fronts move fast, while making it small enough to be computationally manageable in the dense, highly refined regions. This approach may mitigate some of the shortcomings of RSL, in particular with respect to the front speeds in low density regions. However, the validity of RSL nor VSL with respect to predicting the *neutral hydrogen fraction*, has not been much studied before in RSL cosmological simulations, and this is what we aim to investigate in the present paper. In Sec. 3, we present simulations of the epoch of reionization performed with RAMSES-CUDATON using 100%, 20%, 5% and 1% of the speed of light, and show that RSL simulations systematically overpredict the post-reionization neutral hydrogen fraction. We then interpret this result using

analytical arguments and further simulations. We finally close the paper with our conclusions.

## 2. Methodology

### 2.1. Simulations

We used RAMSES-CUDATON (Ocvirk et al. 2016), a coupling between RAMSES (Teyssier 2002) and ATON/CUDATON (Aubert & Teyssier 2008, 2010). Thanks to the CUDA optimization of ATON, RAMSES-CUDATON is able to take advantage of GPU acceleration and routinely performs RHD simulations with the full speed of light. It is therefore an adequate testbed for investigating artefacts in RSL simulations, which are less computationally expensive. The setup used here is a  $4 \text{ h}^{-1}\text{Mpc}$  box discretized on a fixed  $256^3$  grid with parameters similar to the Cosmic Dawn I simulation performed on Titan at Oak Ridge National Laboratory (Ocvirk et al. 2016), but with several differences which we detail here: (i) the cosmology adopted is compatible with Planck 2015 (Planck Collaboration et al. 2015). We have adopted  $\Omega_\Lambda = 0.693$ ,  $\Omega_m = 0.307$ ,  $\Omega_b = 0.048$ ,  $h = 0.677$ , and the power spectrum is described by  $\sigma_8 = 0.8288$ , with an index  $n = 0.963$ , (ii) the fiducial star formation efficiency is  $\epsilon_* = 0.033$ , promoting earlier reionization, (iii) the stellar particle ionizing radiation escape fraction is  $f_{\text{esc}} = 0.1$ , and (iv) the temperature criterion for star formation has been removed, allowing star formation in all cells with a gas density higher than 50 times the average baryon density  $\delta_* = 50 \langle \rho_b \rangle$ . In CoDa II, similar parameters allowed us to reproduce a number of observable constraints of the EoR. Therefore we consider them to be adequate for the purpose of this letter. For our  $4 \text{ h}^{-1}\text{Mpc}$  box, the resulting reionization history is shown as the thick black line in Fig. 1. Although the box successfully reionizes around  $z=6.5$  for our full speed of light run, the timing of reionization is not of great importance for this experiment, since we are more interested in investigating the post-reionization ionized fraction when varying the speed of light.

### 2.2. Reduced speed of light, dual speed of light

The ATON RT module consists of 2 main sub-modules: an advection (i.e. photon propagation) module, and a thermochemistry module, which is purely local and models the interaction between the photons and the hydrogen gas. We will therefore consider the 2 following speeds of light:

- $c_{\text{pr}}$ : the speed of light used in the propagation module,
- $c_{\text{ch}}$ : the speed of light used in the thermochemistry module.

With these definitions, the usual RSL approximation is obtained by using the same reduced speed of light  $c_{\text{rsl}} = c_{\text{pr}} = c_{\text{ch}}$  in both modules. This is the approach of Rosdahl et al. (2013); Trebitsch et al. (2017); Katz et al. (2017) for instance. As we will see, this has a strong impact on the volume-weighted average neutral ionized fraction after reionization. We note that this methodology differs from the one of Gnedin (2016), who distinguish between the radiation background and the fluctuations on top of the latter. In the latter case the reduced speed of light is only used to propagate the fluctuations. We caution that the results presented here may not apply to the latter formulation.

<sup>1</sup> Graphics Processing Units

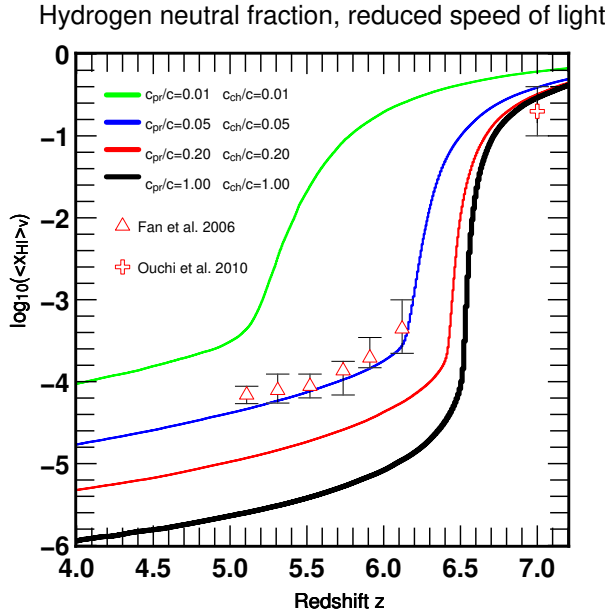


**Fig. 1.** Reionization histories (volume-averaged neutral hydrogen fraction) of our RAMSES-CUDATON simulations in the reduced speed of light approximation.

We also introduce the dual speed of light approximation (hereafter DSL), where the speed of light  $c_{\text{pr}}$  is reduced in the propagation module, but maintained to its true value  $c_{\text{ch}}=c$  in the chemistry module. We performed 1 reference “true” simulation with  $c_{\text{pr}}=c_{\text{ch}}=c$ , 3 RSL simulations with  $c_{\text{pr}}=c_{\text{ch}}=0.2c$ ,  $0.05c$  and  $0.01c$ , respectively. And finally we performed 3 DSL simulations with the true speed of light  $c_{\text{ch}}=1$  in the chemistry module but varying the propagation speed  $c_{\text{pr}}=0.2c$ ,  $0.05c$  and  $0.01c$ . The latter will help us understand the shortcomings of the RSL runs. The results are presented in the next section.

### 3. Results

In this section we examine the impact of the RSL approximation on the post-reionization volume-averaged neutral fraction for different values of the speed of light.

#### 3.1. RSL: reduced speed of light

The reionization histories obtained in the RSL approximation with  $c_{\text{rsl}}=c_{\text{pr}}=c_{\text{ch}}=c$ ,  $0.2c$ ,  $0.05c$  and  $0.01c$  are shown in Fig. 1. The end of reionization, marked by a sudden drop in neutral fraction, is clearly delayed with respect to the true solution (thick black line), although for  $c_{\text{rsl}}=0.1c$  the lag is rather small. These temporal aspects will be studied in more detail in Deparis et al. (2019). Here, instead, we focus on the neutral hydrogen fraction. First of all, our run with the full speed of light yields a neutral fraction in disagreement with the observations of Fan et al. (2006). This is actually commonplace among simulations using the full speed of light (Aubert & Teyssier 2010; Petkova & Springel 2011; So et al. 2014; Bauer et al. 2015; Ocvirk et al. 2016, 2018). We find that the best agreement with Fan et al. (2006) is found for the  $0.05c$  run. This shows that obtaining the correct neutral fraction after overlap in RSL does not guarantee that the correct answer will still be obtained when using

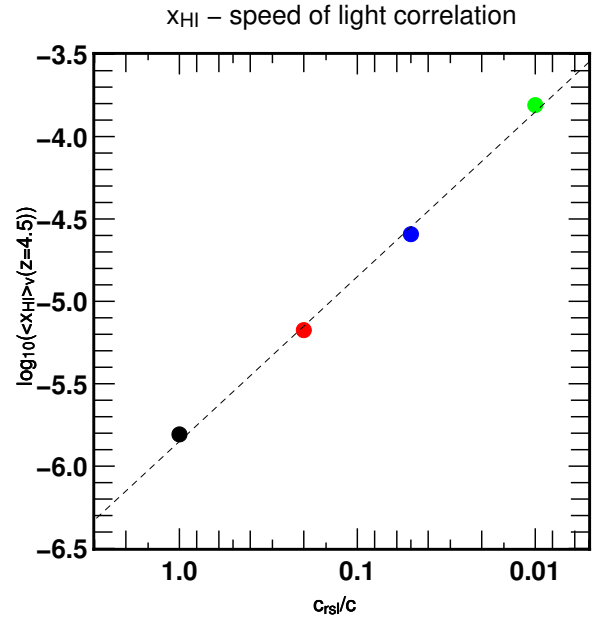


**Fig. 2.** Correlation between the post-overlap volume-weighted neutral fraction (taken at  $z=4.5$ ) and the adopted speed of light in our RSL simulations. The dashed line represents a linear correlation of slope 1.

the full speed of light. However, this doesn't necessarily rule out the use of the reduced speed of light if simulations with different speeds of light converge on a neutral fraction for a given reionization history.

More importantly, we find that the post-reionization average neutral fractions are spread in a wide sequence parameterized by the speed of light, with low speeds of light yielding later reionization and higher neutral fraction.

In all RSL runs, the neutral fraction after reionization is too high compared to the true solution, by a factor  $\sim 5$  ( $\sim 20$ ,  $\sim 100$ ) for  $c_{\text{rsl}}=0.2c$  ( $c_{\text{rsl}}=0.05c$ ,  $c_{\text{rsl}}=0.01c$  respectively). Indeed, this strong quantitative correlation between the adopted speed of light and the post-overlap neutral fraction is shown in Fig. 2. The post-overlap fractions are taken at  $z=4.5$ , where all simulations have completed reionization. The points corresponding to our 4 fiducial RSL form a sequence which is well represented by a linear correlation of slope 1 (dashed line), suggesting that  $c_{\text{rsl}}$  is the main parameter governing the post-overlap neutral fraction in these simulations. We can understand this by considering the analytical expression for the neutral fraction of a hydrogen gas in photo-ionized equilibrium, in the strongly photo-ionized limit (i.e.  $x_{\text{HI}} < 0.01$  for instance). In this case, the neutral fraction behaves as:

$$x_{\text{HI}} \sim \alpha_B \rho_{\text{H}} / c \rho_i \sigma \quad (1)$$

where  $\alpha_B$  is the case B recombination coefficient,  $\rho_{\text{H}}$  is the total hydrogen density,  $\rho_i$  is the ionizing photon density,  $\sigma$  is the ionizing cross-section of hydrogen, and  $c$  is the speed of light. This expression shows that, in this regime, the neutral hydrogen fraction follows an inverse linear dependence with the speed of light  $c$ : dividing  $c$  by a factor 5 results in a neutral fraction increased by the same factor 5 with respect to the true solution using the full speed of light, and this is indeed what we find in the RSL simulations shown in Fig.

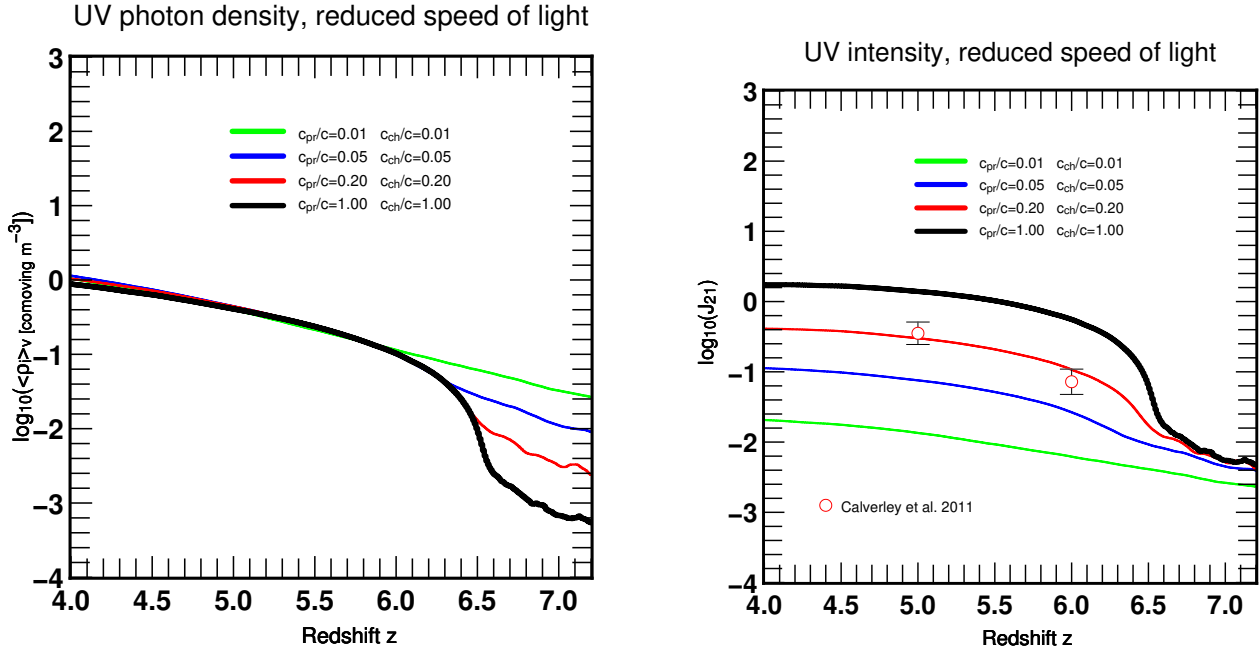


**Fig. 3.** Volume-averaged ionising photon density (left) and ionising intensity (right) for our 4 RSL runs. Note how similar post-reionization ionizing photon densities between the runs translate into different ionizing intensities due to the RSL approximation.

1. The other terms in this expression are subject to only small variations between our simulations:

- The case B recombination coefficient  $\alpha_B(T)$  is a function of temperature, which in our post-reionization IGM, is the temperature of post-reionization photo-ionized hydrogen, i.e. 5 000 - 20 000 K.
- We find an average post-reionization ( $z = 5$ ) ionizing photon density  $\rho_i \sim 0.5$  photon per comoving  $\text{m}^3$  for all RSL runs, as shown in the left panel of Fig. 3.

These 2 parameters are therefore not likely to cause the order of magnitude offsets seen in the RSL runs.

This trend of RSL simulations yielding higher neutral fractions with respect to full speed of light simulations is also seen in the literature, although it has not been clearly identified, explained and reported until now. For instance, this result is similar to the  $z < 6$  region of Fig. 13 of Bauer et al. (2015), hereafter B15, although the authors only comment on the lagging reionization history of their RSL runs.

Since the neutral fraction depends strongly on the local gas density, we expect the speed of light to have less impact in shielded/high density regions. This can be verified using Fig. 4, where we show the ionized fraction of our simulations as a function of gas overdensity for the  $z=4.4$  snapshot. The neutral fraction converge for overdensities larger than  $\sim 1000$ .

Finally, an alternative, but erroneous interpretation of our results could be that the higher neutral fraction of the reduced speed of light runs is a consequence of later reionization: structures would be less ionized because they have spent a shorter time seeing the background. To investigate this possibility we ran a  $c_{\text{rsl}}=1$  simulation with a lower star formation efficiency  $\epsilon_* = 0.02$  than our fiducial models, in order to make reionization happen *after* our fiducial  $c_{\text{rsl}}=0.05$  run. The result is shown in Fig. 5. The obtained reionization history essentially looks like a delayed

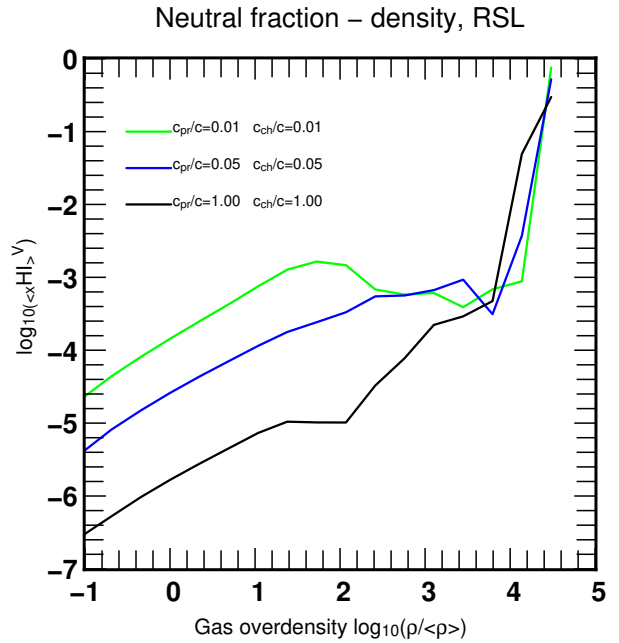


**Fig. 4.** Average neutral fraction as a function of gas density for RSL and full speed of light runs at  $z=4.4$ .

version of our fiducial  $c_{\text{rsl}}=1$  run, horizontally offset by a  $\Delta z = 0.7$  to later times. Although this run reionizes later than the fiducial  $c_{\text{rsl}}=0.05$  run, it still yields a much lower post-overlap neutral fraction. This shows that the offsets in post-overlap neutral fractions between our fiducial runs are not due to offsets in the timing of reionization: even if we re-tune our runs (via e.g. the star formation efficiency as we have done in this example) so as to achieve the same reionization redshift for all  $c_{\text{rsl}}$ , this can not compensate the offsets in post-overlap neutral fractions.

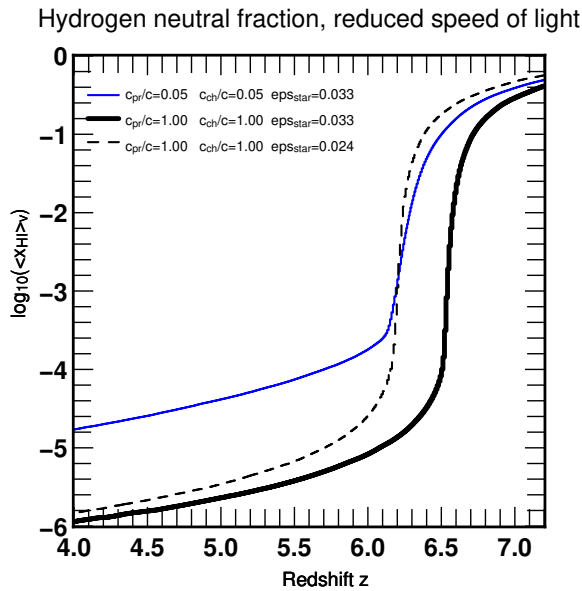


**Fig. 5.** Reionization histories of our fiducial  $c_{\text{rsl}}=0.05$  and  $c_{\text{rsl}}=1$  runs and a  $c_{\text{rsl}}=1$  run with lower star formation efficiency. The lower star formation efficiency delays reionization, but still yields a post-overlap neutral fraction far below that of the reduced speed of light run.

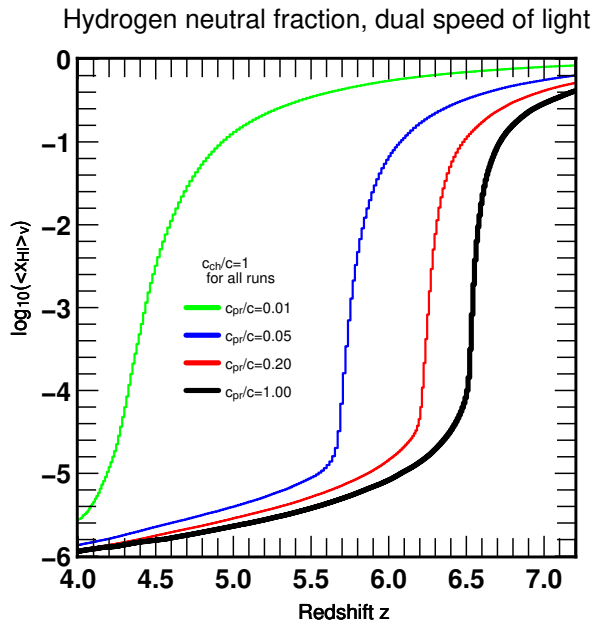


**Fig. 6.** Reionization histories of our Dual speed of light runs.

### 3.2. DSL: dual speed of light

It appears from Eq. 1 that the large error in post-reionization equilibrium fraction obtained with RSL may be entirely due to the use of a reduced speed of light in the thermo-chemistry solver, which is similar to artificially reducing the reaction cross-section, or the photon density. Here we confirm this explanation with 3 additional simulations, using a reduced speed of light in the propagation module  $c_{\text{pr}}=0.2c$ ,  $0.05c$ , and  $0.01c$ , but keeping this time the true speed of light  $c_{\text{ch}}=c$  in the chemistry module. This

setup assumes simultaneously 2 different speeds of light, hence the term “dual speed of light” approximation or DSL.

The resulting reionization histories are shown in Fig. 6. In stark contrast to the RSL runs, the average neutral fractions after reionization converge this time to the true solution, clearly demonstrating that the reduced speed of light in the chemistry solver is indeed the origin of the large overestimate found with RSL.

Although the DSL approximation produces the correct post-reionization neutral fraction, it may well have its own caveats and artifacts. For instance, a slower propagation speed artificially increases the photon density around sources compared to the true speed of light case. In RSL, this is exactly compensated by a reduced speed of light in the photoionization rate, and this is why RSL yields correct neutral fractions for Stromgren spheres, as shown by Rosdahl et al. (2013). Conversely, in DSL, where the photoionization rate uses the true speed of light, the increased photon density produces over-ionized Stromgren spheres. This is illustrated in Fig. 7.

Moreover, Fig. 6 shows that the lag in reionization redshift is even worse in DSL than in RSL. All DSL runs reionize significantly later than their RSL counterpart. The most likely culprit for this is a deficit of star formation in DSL runs compared to the fiducial and RSL runs. This is shown in Fig. 8. In RSL, the box’s SFR is rather close to the fiducial SFR all the way to the overlap, and starts to diverge afterwards, where SFRs split into a sequence ordered by decreasing speeds of light: a slower speed of light results in a higher SFR after overlap. This result can be related to the findings of Dawoodbhoy et al. (2018), who showed using the CoDa I simulation (Ocvirk et al. 2016) that star formation in low mass haloes was reduced by the reionization of their local patch. In our experiment, the increasingly late reionization histories obtained in RSL would therefore trigger this suppression at later times, resulting in the difference found between the full speed of light SFR and RSL SFRs.

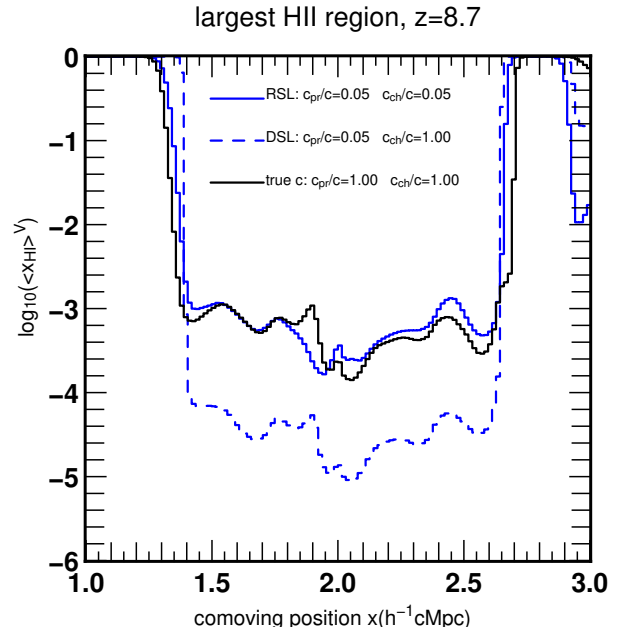


**Fig. 7.** Neutral hydrogen fraction profile around the most massive halo of the simulation at  $z=8.7$ .

Conversely, the DSL runs yield opposite results in both aspects: the SFRs differ *before* overlap and seem to converge *after* overlap, and the sequence of SFRs is ordered in decreasing speeds of light: a slower speed of light results in a lower SFR. This deficit in SFR, in turn, results in a slower reionization history, in particular with the slowest speed of light considered.

This requires a different explanation: we showed in Fig. 7 that DSL yields over-ionized Stromgren spheres, which may hamper cooling and subsequent star formation. Indeed, in pure hydrogen chemistry, neutral hydrogen thermal excitation and subsequent line emission is the main cooling process between  $10^4 - 10^{5.5}$  K (Katz et al. 1996), and the cooling rate involves the product of the neutral hydrogen and electron densities  $\rho_{\text{HI}} \times \rho_e$ , which is maximum at  $x_{\text{HI}} = 0.5$  in a hydrogen-only Universe, and decreases for lower neutral fractions.

We note, though, that the rather strong impact of  $c$  on our SFRs, is exaggerated by the relatively low density threshold for star formation we used: indeed, Fig. 4 shows that our density threshold for star formation is in the range where the neutral fraction is strongly affected by  $c$ . If we could use as star formation threshold a comoving overdensity of  $10^4$ , for instance, where gas is more likely to be neutral according to Fig. 4, it is possible that the impact of  $c$  on the SFR would be less important. However, with such a threshold, star formation would be extremely rare in the setup used here and this would prevent us from obtaining a reasonable reionization history. This approach is therefore not viable here, but may be in a very high resolution simulation.

In the light of our results, we can not at this stage advocate for the use of DSL as a replacement of RSL. The latter will overestimate the average neutral hydrogen fraction in the post-reionization photon bath, while DSL will overestimate the ionization of hydrogen before overlap, while Stromgren spheres are still growing under the influence of local sources. It seems RSL works best before overlap, while DSL is preferable after overlap. Ideally, one would need to switch from one framework to the other along the course of a simulation. A physically motivated scheme for switching from RSL to DSL as a function of the radiative state of a region would be highly desirable but is beyond the scope of this paper.

### 3.3. Resolution study

It is commonly accepted that resolving Lyman-limit systems (hereafter LLSs) is necessary to describe properly the population of absorbers in the IGM and circum-galactic medium (hereafter CGM) and predict the correct average neutral hydrogen fraction (Miralda-Escudé et al. 2000). Therefore spatial resolution is expected to have some impact on the post-overlap neutral fraction. In particular, Rahmati & Schaye (2017) quote a physical size of  $1 - 10$  kpc for Lyman-limit systems, and claim that therefore a spatial resolution of sub-kpc physical is required to describe them. While our fiducial simulations satisfy this constraint at  $z \sim 20$ , they do not satisfy it after overlap: at  $z = 5.5$ , their cell size is about 3.85 physical kpc. Therefore we ran an additional suite of 3 simulations in order to check the impact of physical resolution on our results, where we varied the spatial resolution in a factor of 2 and 4 respectively to our fiducial simulation. The reionization histories of these sim-

ulations are shown in Fig. 9. These new simulations achieve complete reionization between redshifts 6 and 7. However, because the effect we are after is rather small, we shifted their reionization histories to match the reionization redshift of the fiducial run, for better comparison. With this shift applied, they line up perfectly over the overlap period, but produce different tracks after overlap. The neutral fractions of higher spatial resolution simulations are higher than in our fiducial run: each factor of 2 increase in spatial resolution results in an increase of neutral fraction after overlap of about  $\sim 1.4 - 1.6$  with respect to the fiducial run. The exact numbers are reported in Tab. 1.

The boosts in neutral fraction with resolution we find are similar to those obtained by Rahmati & Schaye (2017) in their resolution study. Our most resolved simulation is similar to the L050N0512 and L025N0256 cases of Rahmati & Schaye (2017) in terms of spatial resolution, and therefore reaches the sub-kpc physical spatial resolution constraint stated by these authors even at  $z = 5$ . With this high resolution, which is in principle high enough to resolve LLSs, our neutral fraction is  $\sim 0.35$  dex higher, i.e. a factor of about 2 larger than our fiducial runs. We also show the result of a high resolution RSL simulation with  $c_{\text{pr}} = c_{\text{ch}} = c/0.05$  in Fig. 9, along with its summary results in Tab. 1. Even at this higher resolution, reducing the speed of light still has a strong impact on the post-overlap neutral fraction.

A striking feature of Fig. 9 is that, although the cosmic SFR is increased by  $0.2 - 0.3$  dex at every spatial resolution increment of 2, the neutral fraction also goes up. This is surprising at first sight: an increased SFR means a higher intrinsical ionizing emissivity, and one would therefore expect the average neutral fraction to go down. Yet we find the opposite. In fact, also strikingly, the UV intensity goes down with increasing resolution, despite the increase in SFR, as shown in Fig. 10. How can this be? One may take this as a sign that thanks to increased resolution, LLSs absorbers are either more abundant or more efficient at absorbing the extra radiation (if they have a higher density, and/or a more neutral core). Another possibility is that the ionizing escape fraction becomes smaller at high resolution, thanks to a better description of halo gas. It is impossible to tell which of these effects prevail from this experiment alone. The question, in essence, is whether spatial resolution helps absorbing ionizing photons overall or if it hampers their escape from the production sites.

In order to gain insight into this question and try to disentangle the two possible scenarios we use an additional set of idealized fully coupled radiation-hydrodynamics simulations performed in the context of the “Shining A Light through the dark ages” (hereafter SALT), presented in Appendix A, without star formation, and designed to have exactly the same photon density, imposed by an external incoming radiation field, at all resolutions. They show unambiguously that increasing spatial resolution by a factor even as high as 64 at fixed ionizing intensity only has a very small and short-lived impact on the volume-weighted neutral fraction, demonstrating that improving the description of LLSs has very little impact on that observable.

This may appear to be in contradiction with the results obtained for the L04NXXXX simulations (Tab. 1, CoDa II-like setup, with star formation), where we found that increasing the spatial resolution by just a factor 4 yielded an increase in post-overlap neutral fraction of 0.35 dex. Using

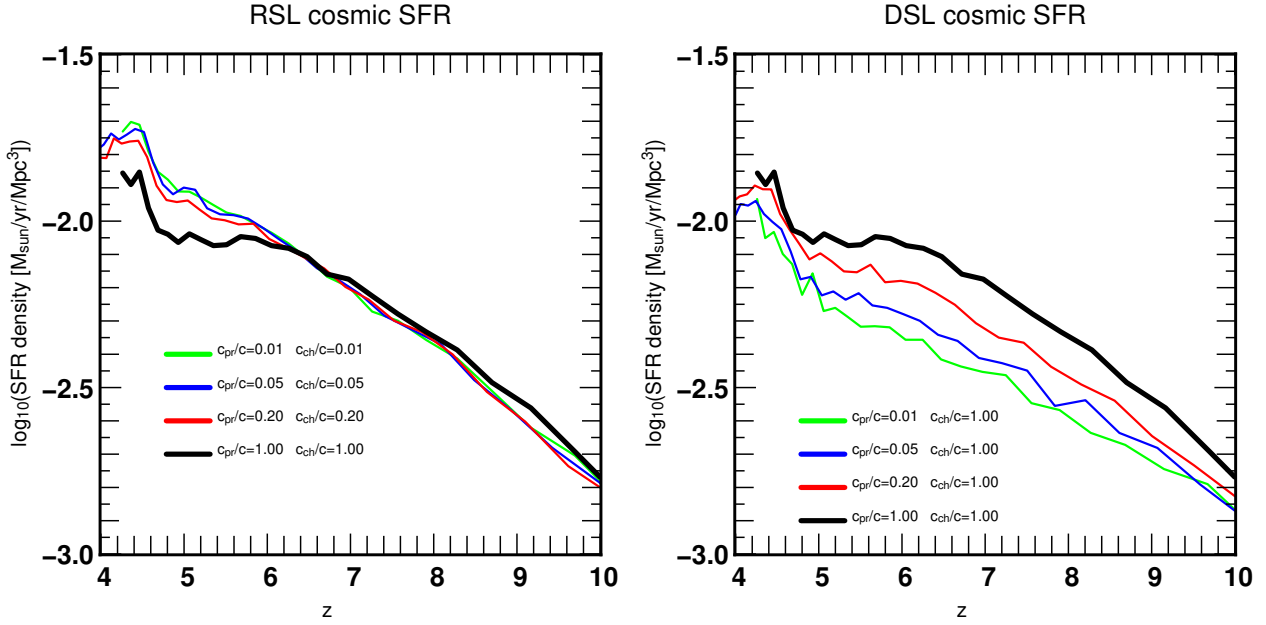


**Fig. 8.** Cosmic star formation rates for the RSL (left) and DSL (right) runs.

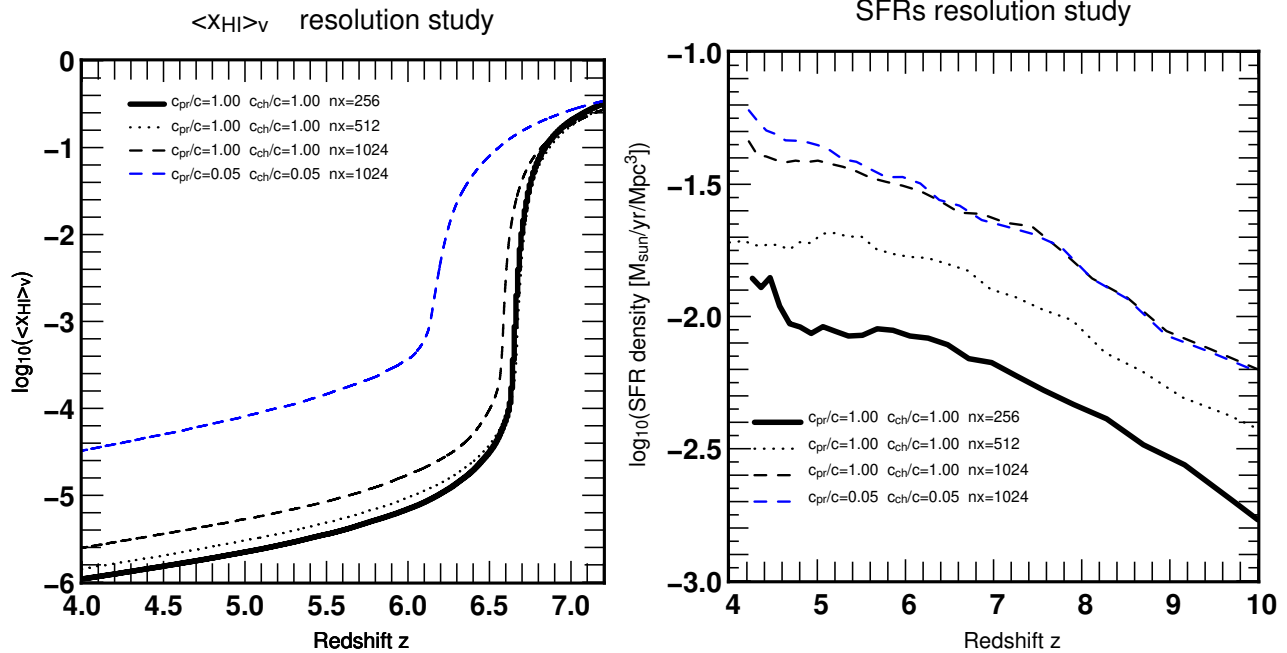


**Fig. 9.** Reionization histories (left) and cosmic star formation rates (right) of  $4 h^{-1} \text{Mpc}$  boxes simulations with spatial resolutions of 1, 2, and 4 times our fiducial resolution. The fiducial run is shown as a thick black line. All runs were calibrated so as to reach  $x_{HI} = 0.5$  between  $z=6$  and  $z=7$ . The detailed properties of these simulations are listed in Tab. 1.

a simple log scaling of the SALT results (maximum 0.3 dex increase in  $x_{HI}$  for a factor 64 increase in resolution), we can estimate that a factor 4 increase in resolution yields only  $0.3/16 = 0.01875$  dex in this setup, much smaller than the 0.35 dex found between the L04N0256 and L04N1024 simulations. This suggests that the increase in post-overlap neutral fraction in Sec. 3.3 is not predominantly due to a better description of LLSs. Instead, the increase in volume-averaged neutral fraction must be due to the lower escape fractions promoted by higher resolution, as was already sug-

gested by the conjoint occurrence of a higher SFR and yet also higher neutral fraction in Fig. 9.

As a conclusion to this resolution study, while spatial resolution indeed impacts our simulations, the volume-weighted average neutral fraction is primarily driven by the decrease of the ionizing escape fraction with increasing resolution.

Simulation	$c_{\text{pr}}/c$	$cN_{\text{DM}}$	$M_{\text{DM}}$	$dx$ (ckpc)	$dx_{\text{phys}}$ (kpc, $z=5$ )	$x_{\text{HI}}(z=5)$	Comment
L04N0256	1	$256^3$	$4.07 \times 10^5 M_{\odot}$	23.08	3.85	$5.59 \times 10^{-6}$	Fiducial
L04N0512	1	$512^3$	$6.21 \times 10^4 M_{\odot}$	11.04	1.84	$3.94 \times 10^{-6}$	$dx_{\text{fiducial}}/2$
L04N1024	1	$1024^3$	$7.77 \times 10^3 M_{\odot}$	5.52	0.92	$2.45 \times 10^{-6}$	$dx_{\text{fiducial}}/4$
L04N1024c005	0.05	$1024^3$	$7.77 \times 10^3 M_{\odot}$	5.52	0.92	$3.23 \times 10^{-5}$	$dx_{\text{fiducial}}/4$

**Table 1.** Summary table of the simulations of our resolution study, giving the number of particles, the dark matter particle mass, the spatial resolution in comoving kpc, and the resulting neutral fraction obtained at  $z=5$ . All simulations are performed with the full speed of light, except for L04N1024c005 which is a RSL simulation with  $c_{\text{pr}}=c_{\text{ch}}=0.05$ .

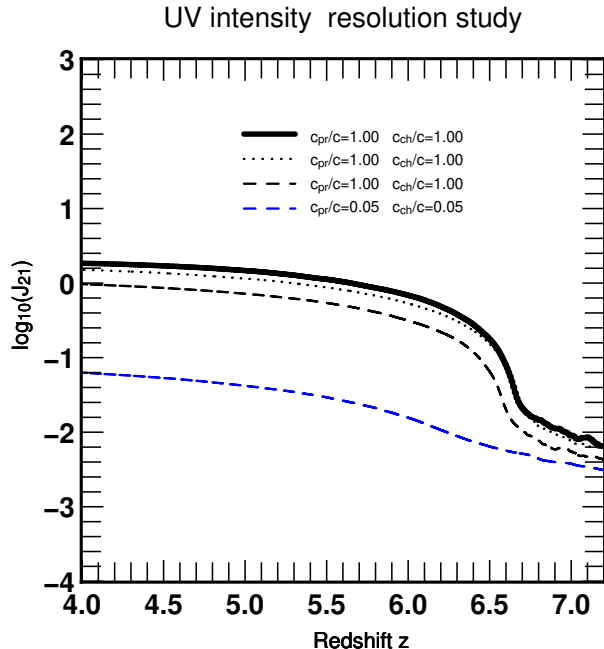


**Fig. 10.** Same as Fig. 9 for the UV intensity.

#### 4. Conclusions

We have investigated the impact of the RSL approximation on the properties of the intergalactic medium using fully coupled radiation-hydrodynamics RAMSES-CUDATON simulations. We find that reducing the speed of light by a factor 5 (20, 100) leads to overestimating the post-reionization neutral hydrogen fraction by the same factor  $\sim 5$  (20, 100, respectively) with respect to our reference simulation using the full speed of light. We consider the simple analytical expression for a hydrogen gas in photo-ionization equilibrium to show that the error is driven by the hydrogen - photon chemistry: reducing the speed of light has the same effect as artificially reducing the reaction cross-section or reducing the photon density, and results in underestimating the ionizing intensity  $J_{21}$ . We confirm this interpretation by running additional simulations using a reduced speed of light in the propagation module, but keeping this time the true speed of light in the chemistry module. With this setup, dubbed “dual speed of light” because of the simultaneous use of 2 different speeds of light, the post-reionization neutral hydrogen fractions converge to the true value, which validates our explanation.

It is important to note that the results presented here apply only to those implementations of RSL where the background is not followed differently from the amplification around sources and does not affect those simulations

using the implementation of Gnedin & Abel (2001). However, for the nonetheless very popular class of radiative transfer implementations on which we have focused here, we have exposed an overlooked, fundamental issue of the reduced speed of light approximation, which should be kept in mind when interpreting results obtained in this framework.

We find that the cosmic SFR or our simulations is impacted by modifications of the speed of light. In RSL, the box’s SFR is rather close to the fiducial SFR all the way to the overlap, and starts to diverge afterwards, where SFRs split into a sequence ordered by decreasing speeds of light: a slower speed of light results in a higher SFR after overlap. Conversely, the DSL runs yield opposite results in both aspects: the SFRs differ *before* overlap and seem to converge *after* overlap, and the sequence of SFRs is ordered in decreasing speeds of light: a slower speed of light results in a lower SFR. However, we caution that this sensitivity to the speed of light may be less acute in simulations using a higher density threshold for star formation.

Later on, after reionization, the neutral fraction governs the properties of the Lyman- $\alpha$  forest and may impact the properties of simulated Lyman- $\alpha$  emitters as well. However, in moderately ionized regions ( $x_{\text{HI}} > 0.1$ ) and for a given photon density, the dependency between  $x_{\text{HI}}$  and the adopted speed of light  $c$  becomes shallower, and in quasi-neutral regions, the equilibrium neutral fraction may become insensitive to the adopted speed of light. Therefore, depending on the exact physical properties of the main absorbers responsible for the Lyman- $\alpha$  forest, they may or may not be affected by the RSL approximation.

We also performed a resolution study, and show that spatial resolution may indeed affects the post-overlap volume-weighted average neutral fraction. However, our results suggest that the predominant effect is via the escape fraction, which appears to decrease as we increase resolution.

As a major goal for the community, it is of prime importance that RHD codes achieve consistent predictions of the volume-weighted average neutral fraction, during and after the end of reionization, because this quantity is often used to calibrate such simulations, although we hope it will be increasingly replaced by a calibration on opacities when possible. Also, since the neutral hydrogen fraction is such an important parameter, we urge all colleagues and authors to always show this quantity rather than, or along with, the average ionized fractions, including after overlap. Moreover, authors should be very careful to properly spell out the type of reduced speed of light approximation used, and its implementation in the photon propagation steps as well as in the thermochemistry module. This information is essential to understand and gauge the significance of the flurry of studies published these recent years and ongoing.

## Acknowledgements

The simulations used in this study were performed on CSCS/Piz Daint (Swiss National Supercomputing Centre), as part of the “Shining a light through the dark ages” PRACE allocation. Auxiliary simulations were performed at the HPC center of the Strasbourg university. The author thanks D. Munro for freely distributing his Yorick programming language<sup>2</sup>

---

<sup>2</sup> <http://www.maumae.net/yorick/doc/index.html>

## Appendix A: Idealized simulations

As an additional resolution study we present here results from a new suite of simulations performed under the “Shining A Light Through the dark ages” (hereafter SALT simulations). The purpose of these simulations in this paper is to quantify the impact of spatial resolution on the volume-weighted average neutral fraction with an emphasis on isolating the influence of better resolving LLSs while leaving out the possible impact of escape fraction variations also due to spatial resolution. For this reason, these simulations are idealized: they have no star formation, therefore no internal source of radiation, and no supernova feedback. The only source of radiation is an external background entering the domain through the left boundary.

These simulations will be described and analysed more extensively in a forthcoming paper, and we therefore here only outline their main properties. The SALT simulations were performed using RAMSES-CUDATON on Piz Daint (CSCS), using up to 2048 nodes in parallel. The cosmology is the same as CoDa II (Ocvirk et al. 2018) and the simulations presented above. The computational domain is a  $1h^{-1}\text{Mpc}$  box, discretized on grids with a resolution of  $2048^3$ ,  $1024^3$ ,  $512^3$ , down to  $32^3$ . The physics are the same as CoDa II, except that there is no star formation. The SALT simulations are designed to study the evolution of a patch of Universe undergoing irradiation by an external source during the onset of the epoch of reionization: at  $z=10$ , a flux  $F_0$ , as defined in Iliev et al. (2006), enters the box from the left side, giving rise to an ionization front, which travels through the box, reionizing it. All runs receive the same ionizing flux. Radiation enters from the left side of the box but is allowed to freely fly out through all other sides of the domain. The simplicity of the setup allows us to reach very high spatial resolution uniformly, using the full speed of light. Indeed, our most resolved simulation reaches sub-kpc resolution with a physical cell size  $dx=0.1$  kpc at  $z=6$ , which is well within the sub-kpc requirement of Rahmati & Schaye (2017). The results of our runs with increasing spatial resolution are shown in Fig. A.1. The left panel shows the volume-weighted average neutral fraction. The external source is turned on at  $z=10$ , and the neutral fraction evolves quickly as the ionization front crosses the box. Complete reionization is achieved at  $z \sim 9$ , where the volume-weighted neutral fraction reaches  $x_{\text{HI}} \sim 3.10^{-4}$ , and from there decreases slowly. While the results for these runs look very similar, a number of aspects can be highlighted:

- Low resolution runs reionize faster, i.e. the drop in neutral fraction between  $z=10$  and  $z=9$  and is steeper.
- Low resolution runs reach slightly smaller neutral fraction directly after overlap at  $z=9$ . At  $z=8.5$ , the difference between the highest and lowest resolution run is  $\sim 0.3$  dex.
- However, at  $z < 9$ , the neutral fractions seem to converge, and the gap between in  $x_{\text{HI}}$  between the runs vanishes.

These results suggest that spatial resolution may indeed affect absorbers shortly after overlap, and as a consequence, high resolution runs have a higher neutral fraction just after overlap. However, the impact on the volume-weighted neutral fraction is pretty mild, in particular when compared to the impact of resolution on the mass-weighted neutral

fraction, shown in the right panel of Fig. A.1. The mass-weighted neutral fraction remains much higher in high resolution runs, due to the ability of better-resolved, higher density structures to self-shield and resist ionization and photo-evaporation. While we expect spatial resolution to have some impact on how absorbers resist photo-evaporation, we can see that the volume-weighted average hydrogen neutral fraction does not trace this effect in a strong way, because the total volume of these absorbers remains small.

As a further consequence, the ionizing intensity is almost unchanged by the increased spatial resolution, as shown in Fig. A.2. All runs converge to an almost identical value of  $J_{21}$ . The only difference between our runs is the time taken to reach that stationary  $J_{21}$ , which is shorter at low resolution, confirming our previous analysis of the evolution of the neutral fractions.

The post-overlap neutral fraction varies by a factor  $\sim 2$  (i.e. 0.3 dex), when the spatial resolution varies by a factor 64. This is a rather small effect for such a huge range in spatial resolution. To really gauge the impact of spatial resolution on lastingly self-shielding structures requires other tracers, such as halo gas outflow rates, and this will be the focus of a forthcoming paper. As a minor caveat, we remind the reader that these simulations are designed to study the irradiation of a small patch of universe at very high redshift, during the onset of reionization. Therefore, one may criticize the fact that the incident flux is turned on at  $z=10$ , and not at  $z=6$  for instance, where structures would have had more time to form. We note that running such an idealised setup while turning on the external source at  $z=6$  would make less sense because sources within the box would already have started to shine.

## References

Aubert D., Deparis N., Ocvirk P., 2015, MNRAS, 454, 1012  
 Aubert D., Deparis N., Ocvirk P., Shapiro P. R., Iliev I. T., Yepes G., Gottlöber S., Hoffman Y., Teyssier R., 2018, ApJ, 856, L22  
 Aubert D., Teyssier R., 2008, MNRAS, 387, 295  
 Aubert D., Teyssier R., 2010, ApJ, 724, 244  
 Audit E., Charrier P., Chièze J. , Dubroca B., 2002, arXiv Astrophysics e-prints  
 Baek S., Di Matteo P., Semelin B., Combes F., Revaz Y., 2009, A&A, 495, 389  
 Bauer A., Springel V., Vogelsberger M., Genel S., Torrey P., Sijacki D., Nelson D., Hernquist L., 2015, MNRAS, 453, 3593  
 Butler M. J., Tan J. C., Teyssier R., Rosdahl J., Van Loo S., Nickerson S., 2017, ApJ, 841, 82  
 Costa T., Rosdahl J., Sijacki D., Haehnelt M. G., 2018, MNRAS, 473, 4197  
 Dawoodbhoy T., Shapiro P. R., Ocvirk P., Aubert D., Gillet N., Choi J.-H., Iliev I. T., Teyssier R., Yepes G., Gottlöber S., D’Aloisio A., Park H., Hoffman Y., 2018, MNRAS, 480, 1740  
 Deparis N., Aubert D., Ocvirk P., Chardin J., Lewis J., 2019, A&A, 622, A142  
 Dubroca B., Feugeas J., 1999, Academie des Sciences Paris Comptes Rendus Serie Sciences Mathématiques, 329, 915  
 Fan X., Strauss M. A., Becker R. H., White R. L., Gunn J. E., Knapp G. R., Richards G. T., Schneider D. P., Brinkmann J., Fukugita M., 2006, AJ, 132, 117  
 Gavagnin E., Bleuler A., Rosdahl J., Teyssier R., 2017, MNRAS, 472, 4155  
 Geen S., Hennebelle P., Tremblin P., Rosdahl J., 2016, MNRAS, 463, 3129  
 Gillet N., Ocvirk P., Aubert D., Knebe A., Libeskind N., Yepes G., Gottlöber S., Hoffman Y., 2015, ApJ, 800, 34  
 Gnedin N. Y., 2016, ApJ, 833, 66  
 Gnedin N. Y., Abel T., 2001, New A, 6, 437  
 González M., Audit E., Huynh P., 2007, A&A, 464, 429  
 Iliev I. T., Mellema G., Pen U.-L., Merz H., Shapiro P. R., Alvarez M. A., 2006, MNRAS, 369, 1625

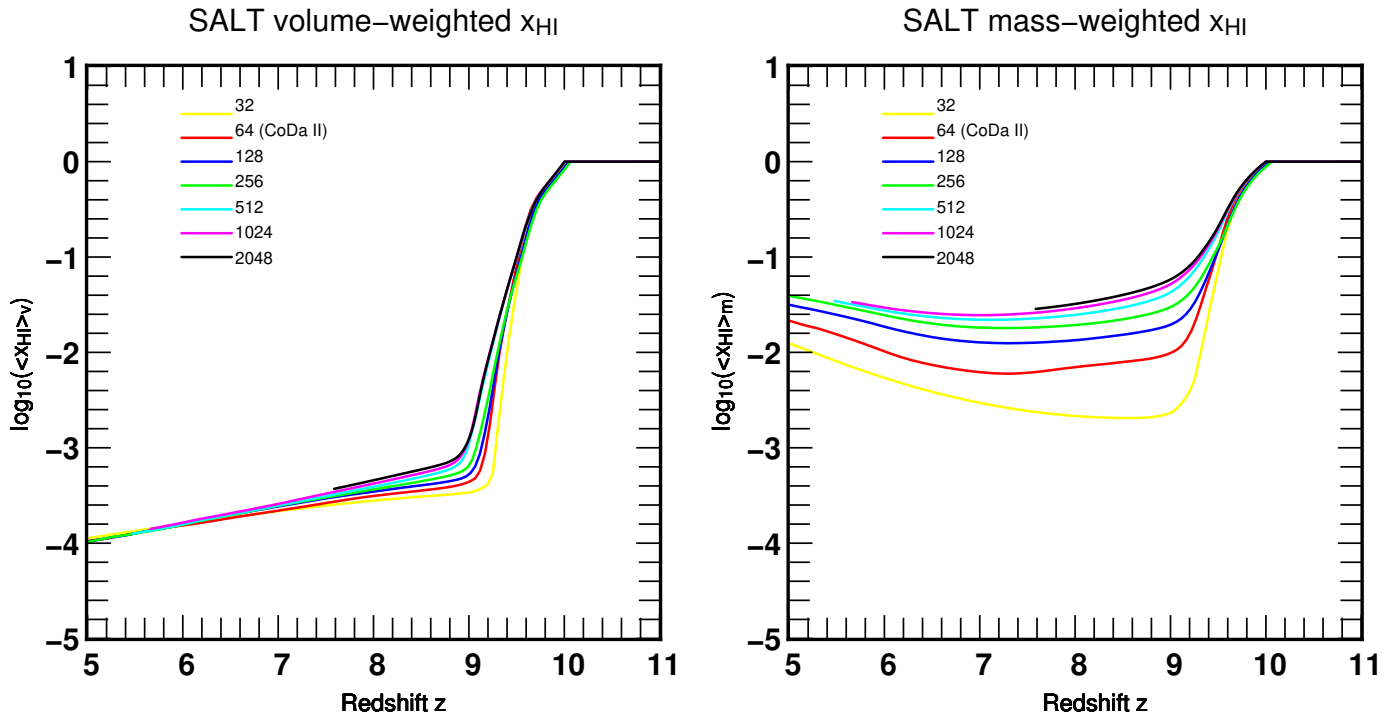


**Fig. A.1.** SALT Resolution study: reionization histories of  $1 \text{ h}^{-1} \text{Mpc}$  boxes idealised simulations performed on grids of  $2048^3$  to  $32^3$ . Left (right): volume-weighted (mass-weighted) average neutral hydrogen fraction. The source is turned on at  $z=10$  for all simulations.

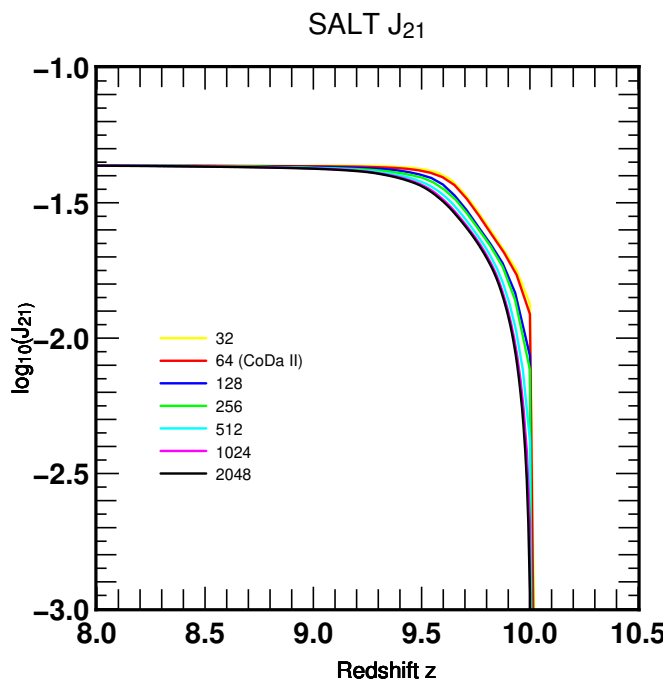


**Fig. A.2.** Same as Fig. A.1 for the ionizing intensity  $J_{21}$ . Note the different redshift limits.

Ocvirk P., Aubert D., 2011, MNRAS, 417, L93  
 Ocvirk P., Aubert D., Chardin J., Knebe A., Libeskind N., Gottlöber S., Yepes G., Hoffman Y., 2013, ApJ, 777, 51  
 Ocvirk P., Aubert D., Sorce J. G., Shapiro P. R., Deparis N., Da-woodbhoy T., Lewis J., Teyssier R., Yepes G., Gottlöber S., Ahn K., Iliev I. T., Hoffman Y., 2018, arXiv e-prints  
 Ocvirk P., Gillet N., Aubert D., Knebe A., Libeskind N., Chardin J., Gottlöber S., Yepes G., Hoffman Y., 2014, ApJ, 794, 20  
 Ocvirk P., Gillet N., Shapiro P. R., Aubert D., Iliev I. T., Teyssier R., Yepes G., Choi J.-H., Sullivan D., Knebe A., Gottlöber S., D'Aloisio A., Park H., Hoffman Y., Stranex T., 2016, MNRAS, 463, 1462  
 Pawlik A. H., Schaye J., 2008, MNRAS, 389, 651  
 Petkova M., Springel V., 2011, MNRAS, 412, 935  
 Planck Collaboration Ade P. A. R., Aghanim N., Arnaud M., Ash-  
 down M., Aumont J., Baccigalupi C., Banday A. J., Barreiro R. B.,  
 Bartlett J. G., et al. 2015, ArXiv e-prints  
 Rahmati A., Schaye J., 2017, ArXiv e-prints  
 Ripoll J.-F., Dubroca B., Duffa G., 2001, Combustion Theory and  
 Modelling, 5, 261  
 Rosdahl J., Blaizot J., Aubert D., Stranex T., Teyssier R., 2013, MN-  
 RAS, 436, 2188  
 Rosdahl J., Katz H., Blaizot J., Kimm T., Michel-Dansac L., Garel T., Haehnelt M., Ocvirk P., Teyssier R., 2018, MNRAS, 479, 994  
 Semelin B., Combes F., Baek S., 2007, A&A, 474, 365  
 So G. C., Norman M. L., Reynolds D. R., Wise J. H., 2014, ApJ, 789,  
 149  
 Teyssier R., 2002, A&A, 385, 337  
 Trebitsch M., Blaizot J., Rosdahl J., Devriendt J., Slyz A., 2017, MN-  
 RAS, 470, 224

Katz H., Kimm T., Haehnelt M., Sijacki D., Rosdahl J., Blaizot J., 2018, ArXiv e-prints  
 Katz H., Kimm T., Sijacki D., Haehnelt M. G., 2017, MNRAS, 468,  
 4831  
 Katz N., Weinberg D. H., Hernquist L., 1996, ApJS, 105, 19  
 Kimm T., Cen R., 2013, ApJ, 776, 35  
 Levermore C. D., 1984, J. Quant. Spectr. Rad. Transf., 31, 149  
 Miralda-Escudé J., Haehnelt M., Rees M. J., 2000, ApJ, 530, 1